

Vortex fluctuations in superconducting $La_{2-x}Sr_xCuO_{4+\delta}$

Yung M. Huh and D. K. Finnemore

Ames Laboratory, USDOE and Department of Physics and Astronomy,
Iowa State University, Ames, IA 50011

(November 3, 2018)

Vortex fluctuations in the $La_{2-x}Sr_xCuO_{4+\delta}$ system have been studied as a function of magnetic field, temperature and carrier concentration in order to determine the dimensionality of the fluctuations. For a $x = 0.10$ sample, there is a unique crossing-temperature on the magnetization vs. temperature plots for all magnetic fields up to $7 T$, and the data scale very well with 2D fluctuation theory. At lower x -values where H_{c2} is much smaller, there are two well defined crossing points, one at low fields (typically less than $1 T$) and another at high fields (typically $3-7 T$). A fit of the data to fluctuation theory shows that the low field crossing data scale as 2D fluctuations and the high field crossing data scale as 3D fluctuations. It would appear that as the magnetic field approaches H_{c2} , there is a 2D to 3D cross-over where the low field 2D pancake vortex structure transforms into a 3D vortex structure.

74.30.Ci., 74.30.Ek, 74.40.+k, 74.60.-w, 74.70.Vy

I. INTRODUCTION

The existence of vortex fluctuations close to the superconducting transition temperature, T_c , in the high temperature superconductors was reported by Kes and coworkers,¹ and theoretical work by Bulaevskii and coworkers² indicated that entropy terms associated with moving vortices could provide a way to understand the unique crossing-point in the magnetization vs. temperature plots that are observed. Early work² focussed on the fluctuation of 2D pancake vortices in materials with a very high anisotropy ratio of the effective mass of the electrons, $\gamma = \sqrt{m_c/m_{ab}}$. Subsequent experimental and theoretical work by Tesanovic and coworkers³ and Welp and coworkers⁴ indicated that the similar crossing-point effects also occur in materials with smaller γ -values, but the fluctuations may have 3D character. In the case of 2D fluctuations, the magnetization scales to a universal curve when the data are plotted as $4\pi M/(TH)^{1/2}$ vs. $[T - T_c(H)]/(TH)^{1/2}$. In the case of 3D fluctuations, the magnetization scales to a universal curve when the data are plotted as $4\pi M/(TH)^{2/3}$ vs. $[T - T_c(H)]/(TH)^{2/3}$. These scaling laws provide an easy test to determine whether the fluctuations have a 2D or 3D character.

A recent study of vortex fluctuations in an underdoped $YBa_2Cu_3O_{6.5}$ sample by Poddar and coworkers⁵ has indicated that there were two distinct crossing points for different magnetic field ranges. Data from $0.2 T$ to $0.75 T$ show a crossing point at $45.2 K$ and 3D scaling. Data from $1.5 T$ to $3.5 T$ show a crossing point at $42.8 K$

and 2D scaling. Theoretical analysis to explain these data⁶ uses a Josephson interlayer coupling Hamiltonian that gives 2D behavior if the ratio of the c-axis coherence distance to copper oxide plane spacing, ξ_c/d , is much less than 1 and 3D behavior if ξ_c/d is substantially more than one. For the Poddar and coworkers sample,⁵ the ratio of the crossing temperature to transition temperature is $T_{3D}^*/T_{co} = [43.4 K/45.15 K] = 0.961$ and $T_{2D}^*/T_{co} = [42.8 K/45.15 K] = 0.948$.

Several types of behavior seem to occur. For a highly anisotropic superconductor like $Bi_2Sr_2Ca_1Cu_2O_{8+\delta}$ ¹ where the critical field at zero temperature, $H_{c2}(0)$, is much larger than the measuring field, the magnetization vs. temperature curves, $4\pi M$ vs. T , have a single well defined crossing-point, T^* and the fluctuations have 2D character. For a more isotropic superconductor like optimally doped $YBa_2Cu_3O_{6.95}$,⁴ there also is a single well defined T^* and the fluctuations have 3D character. For underdoped $YBa_2Cu_3O_{6.65}$,⁵ there can be more than one crossing-point and a cross-over from 2D to 3D behavior. The purpose to the work reported here is to systematically study the change in fluctuations that occur as the doping level is decreased in $La_{2-x}Sr_xCuO_{4+\delta}$ to look for a systematic transformation from 3D to 2D character and to look for the values of reduced magnetic field, $H/H_{c2}(T = 0)$ where this cross-over occurs.

II. EXPERIMENT

The samples used in this work are the same grain-aligned powders and single crystals that were used for measurements of the thermodynamic critical field.⁷ Powders were ground to a particle size less than $20 \mu m$, placed in a low viscosity epoxy and aligned in a field of $8 T$. After the epoxy hardened, X-ray rocking curves showed a full width at half maximum for the (008) peak of 5° . Magnetization studies were made with a Quantum Designs magnetometer.⁷ In all of the scaling analyses presented here, the magnetic field dependent transition temperature, $T_c(H)$ is taken from the Hao-Clem analyses of thermodynamic data presented previously.^{7,8} A full discussion comparing different assumptions for $T_c(H)$ is given elsewhere.⁹

III. RESULTS AND DISCUSSION

As reported earlier,⁸ the magnetization vs temperature curves for the $x = 0.10$ single crystal with $T_{co} = 26.8$ K showed a single crossing point at $T^* = 22.0$ K and $4\pi M^* = -1.13$ G for all data from 1.0 – 7.0 T. No extensive study was made at lower fields. Fits of these data on a $4\pi M/(TH)^{1/2}$ vs. $[T - T_c(H)]/(TH)^{1/2}$ plot show 2D scaling over this entire field range. To discuss the case where the crossings occur at different temperatures, we define a new variable T_{cr} as the temperature where two successive $4\pi M$ vs. T curves cross and plot T_{cr} as a function of magnetic field to show how the crossing point changes with field.

Data for a sample close to optimum doping at $x = 0.143$ are presented in Fig. 1. The data from 0.50 T to 0.95 T cross at about 36.8 K and the data from 2 T to 7 T cross at about 35.4 K, in a manner similar to the $YBa_2Cu_3O_{6.65}$ data reported by Poddar.⁵ These temperatures are fairly close to one another, but they are easily resolved. If data for these two samples are fit to both 2D and 3D scaling, the 3D scaling gives a significantly better fit than the 2D scaling for both plateaus. The data on Fig. 2 for the two samples close to optimum doping, $x = 0.156$ (open stars) and $x = 0.143$, (solid pentagons) are very similar. Within the theory of Rosenstein et al.⁶ the relevant quantity to determine the scaling dimensionality is $b = H/H_{c2}(0)$. For these samples close to optimum doping, the upper critical field, $H_{c2}(0)$, is approximately 33 T, so the measurements up to 7 T never probe the region close to $H_{c2}(0)$ so the $b = H/H_{c2}(0)$ is small. Data for the $x = 0.10$ single crystal shown by the solid triangles in Fig. 2, show that T_{cr} drops smoothly with field and forms a plateau at $T^* = 22.0$ K as reported earlier.⁸ For this sample, fits to both 2D and 3D scaling give a rather good fit to 2D scaling⁸, but a poor fit to 3D scaling. For this $x = 0.10$ sample, $H_{c2}(0) = 34$ T is much higher than the measuring field of 7 T, so the data never approach the upper critical field. The difference between the $x = 0.143$ sample and the $x = 0.10$ sample is that the optimum doped sample obeys 3D scaling and the underdoped sample obeys 2D scaling. This would imply that the c-axis coherence distance to copper oxide plane spacing, ξ_c/d , is always less than one for the magnetic fields measured.

Data for an $x = 0.117$ sample are shown by the solid diamonds on Fig.2. The T_{cr} data are similar to the $x = 0.10$ sample and show 2D behavior over the range measured. For this sample, $H_{c2}(0) = 32$ T, so the measurements up to 7 T do not probe anywhere close to $H_{c2}(0)$.

In the far underdoped region, data for the $x = 0.081$ and $x = 0.070$ samples differ from the above cases in that the respective upper critical fields of $H_{c2}(0) = 11$ T and $H_{c2}(0) = 6$ T are much closer to the top measuring field of 7 T. The $4\pi M$ vs. T data for the $x = 0.081$ sample presented in Fig. 3 show a low field crossing-point at 19.6 K and a high field crossing point at 22.7 K Present-

ing these data on the T_{cr} vs. $\mu_o H$ plot of Fig. 4 shows that the $x = 0.081$ sample (open squares) has a plateau from about 0.3 to 1.0 T, and it has a second plateau from about 3 to 7 T with a gradual transition from 1 – 3 T. Here, data on the low field plateau fit best to 2D scaling, and data on the high field plateau fit best to 3D scaling as shown in Fig. 5a and Fig. 5b. In a similar manner, data for the $x = 0.070$ sample (solid circles in Fig. 4) shows both a low field plateau at 14.2 K and a high field plateau at 15.2 K. Here again, the low field plateau data fit 2D scaling and the high field plateau data fit 3D scaling as shown by Fig. 5c and Fig. 5d. Both these samples show that with an increasing magnetic field, the sample undergoes a cross-over from 2D scaling to 3D scaling as H_{c2} is approached.

To be a bit more quantitative about the 2D to 3D cross-over, we plot the Rosenstein et al. parameters⁶ vs. magnetic field. Within this model, if

$$\xi_c/d \ll 1/2[\sqrt{(b+t-1)^2 + 4bt} + (b+t-1)] = f^{2D}, \quad (1)$$

then one expects 2D scaling. Here, ξ_c is the c-axis coherence distance, d is the copper oxide plane spacing, $b = H/H_{c2}(0)$, and $t = T/T_{co}$. Similarly, within this model, if

$$\xi_c/d \gg b+t-1 + [2(b+t-1)^3]/27 = f^{3D}, \quad (2)$$

then one expects 3D scaling. It should be pointed out that⁶

$$b+t-1 = [T - T_c(H)]/T_c.$$

so this variable measures the reduced temperature interval from the H_{c2} line.

Both f^{2D} and f^{3D} are plotted vs. $\mu_o H$ for each crossing-point, T_{cr} in the insets of Fig. 4 for the $x = 0.081$ and 0.070 samples. From the plot of f^{2D} (open triangles in both insets), it is clear that the region of 3D scaling begins at a magnetic field where f^{2D} becomes as large as 1.0. The f^{3D} functions are also plotted for completeness. These magnetization data do not provide a measure of ξ_c , but it is of interest to note that 3D scaling begins at a magnetic field where the Rosenstein et al. f^{2D} function⁶ reaches 1.0 for both $x = 0.081$ and $x = 0.070$ samples.

IV. CONCLUSIONS

The $La_{2-x}Sr_xCuO_{4+\delta}$ high temperature superconductor system provides a rich arena to study vortex fluctuations. Near optimum doping the $x = 0.143$ and $x = 0.156$ samples show 3D fluctuations over the entire magnetic field range studied. The c-axis coupling is strong enough in the optimally doped samples to make

the fluctuations $3D$ at all the measured fields. Stated another way, ξ_c/d is greater than one for these samples. As discussed previously⁸ a reduction of carrier concentration tends to make the material more $2D$ at magnetic fields substantially below $H_{c2}(0)$, presumably because the relatively weak c -axis coupling in these cuprates is made even weaker with depleted carrier concentration. Reduction of the doping to $x = 0.117$ and $x = 0.10$ gave samples that showed $2D$ fluctuations for all magnetic fields up to $7 T$. Presumably the f^{2D} did not get large enough for fields up to $7 T$ in these two samples to cause a $2D$ to $3D$ transition. For all four of these samples, $H_{c2}(0)$ was over $30 T$ so the $b = H/H_{c2}(0)$ values are small compared to the reduced temperature, $t = T/T_c$ terms and thus the b term in Eq. (1) does not make a large enough contribution to cause the cross-over. With further reduction in doping to $x = 0.081$ and $x = 0.070$, the data probes fields comparable to $H_{c2}(0)$. Then the $b = H/H_{c2}(0)$ term in Eq. (1) is important, as shown in the inset of Fig. 4, and a clear cross-over from $2D$ to $3D$ behavior was seen.

The YBCO and $La_{2-x}Sr_xCuO_{4+\delta}$ data differ in one important respect. The YBCO data^{5,6} show $3D$ behavior at lower fields and $2D$ behavior at higher fields, whereas these $La_{2-x}Sr_xCuO_{4+\delta}$ data show $2D$ behavior at low field and $3D$ behavior at high field. The authors do not understand this difference, but in light of Eq. (1) and the data in the inset in Fig. 4, the $2D$ to $3D$ cross-over with increasing field seems to be a reasonable result.

V. ACKNOWLEDGMENTS

Comments from V. G. Kogan and J. R. Clem were very helpful. Ames Laboratory is operated for the U. S. Department of Energy by Iowa State University under contract No. W-7405-ENG-82 and supported by the DOE, the Office of Basic Energy Sciences.

⁶ B. Rosenstein, B. Ya. Shapiro, R. Prozorov, A. Shaulov, and Y. Yeshurun, Phys. Rev. B **63**, 13450 (2001).

⁷ Y. M. Huh, and D. K. Finnemore, Phys. Rev B (submitted).

⁸ Y. M. Huh, J. E. Ostenson, F. Borsa, V. G. Kogan, D. K. Finnemore, A. Vietkin, A. Revcolevschi, and M. -H. Julien, Phys. Rev. B **63**, 64512 (2001).

⁹ Y. M. Huh, Ph.D. Thesis, Iowa State University, 2001

FIG. 1. Magnetization vs temperature plot for an $x = 0.143$ sample near optimum doping. The crossing point changes as the field increases from $0.95 T$ to $2.0 T$.

FIG. 2. Magnetization crossing points for two successive fields, T_{cr} , as a function of field.

FIG. 3. $4\pi M$ vs. T data for the $x = 0.081$ sample showing two distinct crossing-points for the low field and high field regions.

FIG. 4. Comparison of the plateau regions for T_{cr} with the values of the theoretical f^{2D} and f^{3D} parameters for the (a) $x = 0.081$ and (b) $x = 0.070$ samples.

FIG. 5. $2D$ and $3D$ scaling plots for the two plateaus of the $x = 0.081$ (a, b) and the $x = 0.070$ samples (c, d).

¹ P. H. Kes, C. J. van der Beek, M. P. Maley, M. E. McHenry, D. A. Huse, M. J. Menken, and A. A. Menovsky, Phys. Rev. Lett. **67**, 2383 (1991).

² L. N. Bulaevskii, M. Ledvij, and V. G. Kogan, Phys. Rev. Lett. **68**, 3773 (1992).

³ Z. Tesanovic, L. Xing, L. Bulaevskii, Qiang Li, and M. Suenaga, Phys. Rev. Lett. **69**, 3563 (1992).

⁴ U. Welp, W. K. Kwok, R. A. Klemm, V. M. Vinokur, J. Downey, and G. W. Crabtree, Physica C **185-189**, 1785 (1991); U. Welp, S. Fleshler, W. K. Kwok, R. A. Klemm, V. M. Vinokur, J. Downey, B. Veal, and G. W. Crabtree, Phys. Rev. Lett. **67**, 3180 (1991).

⁵ A. Poddar, R. Prozorov, Y. Wolfus, M. Ghinovker, B. Ya. Shapiro, A. Shaulov, and Y. Yeshurun, Physica C **282-287**, 1299 (1997).

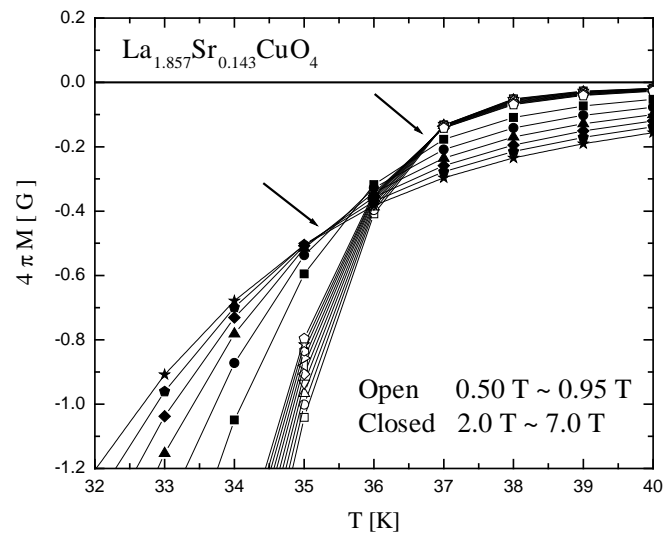


FIG. 1

Yung M. Huh and D. K. Finnemore

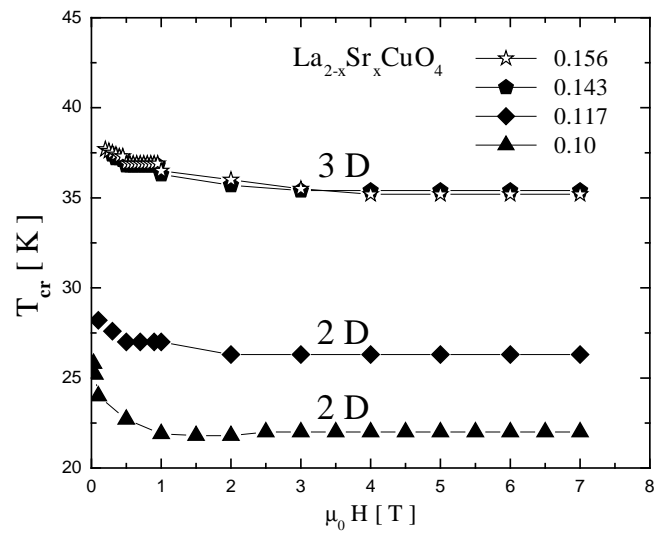


FIG. 2

Yung M. Huh and D. K. Finnemore

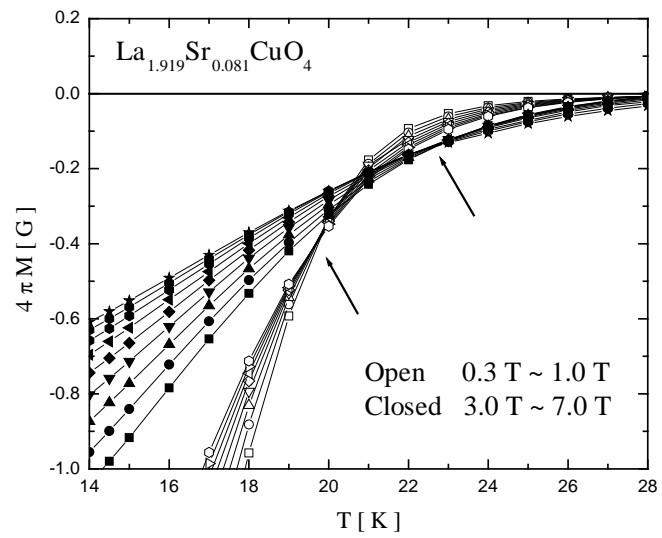


FIG. 3

Yung M. Huh and D. K. Finnemore

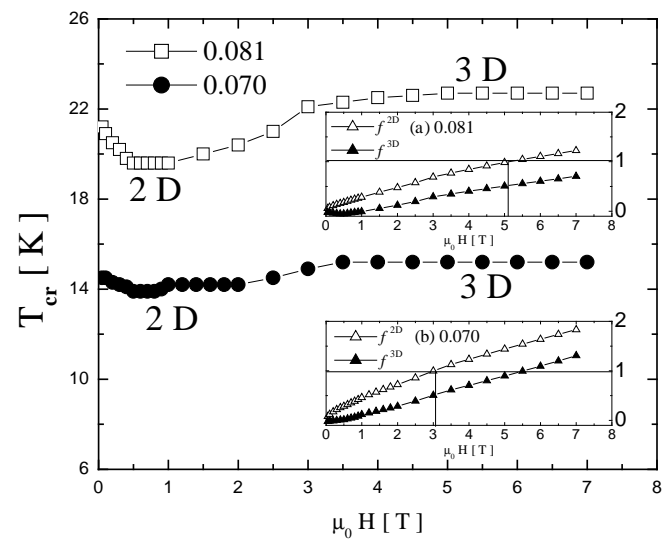


FIG. 4

Yung M. Huh and D. K. Finnemore

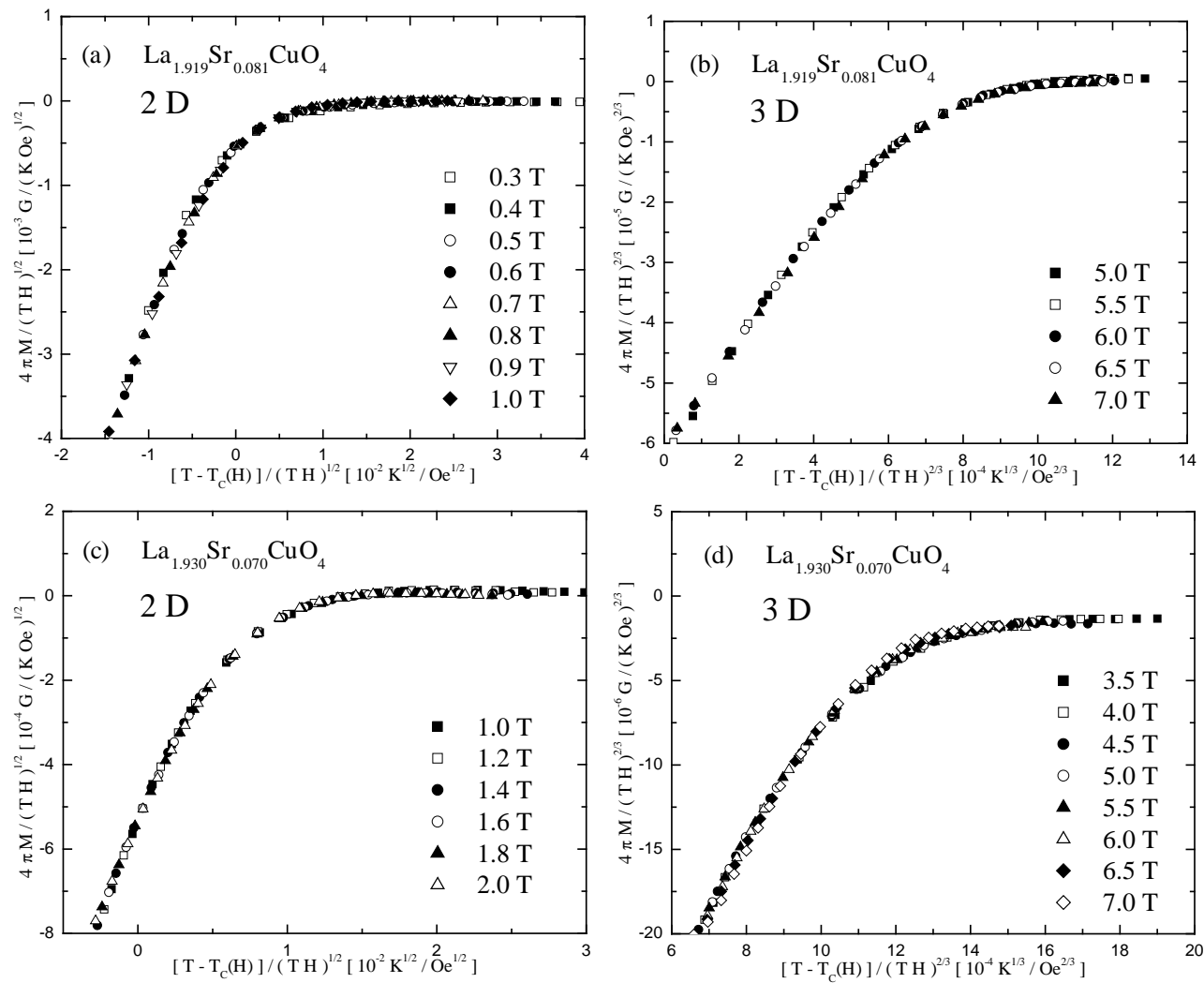


FIG. 5

Yung M. Huh and D. K. Finnemore